

A laminar-jet-discharging method for measuring the interfacial tension of deformable surfaces

Dongmei Wan^{1,2}, Hengsheng Xiang^{1,2} and Haitao Xu^{1,3,4}

¹ Center for Combustion Energy, Tsinghua University, 100084 Beijing, People's Republic of China

² Department of Energy and Power Engineering, Tsinghua University, 100084 Beijing, People's Republic of China

³ School of Aerospace Engineering, Tsinghua University, 100084 Beijing, People's Republic of China

E-mail: wdm16@mails.tsinghua.edu.cn (Dongmei Wan), xhs17@mails.tsinghua.edu.cn (Hengsheng Xiang) and hxu@tsinghua.edu.cn (Haitao Xu)

Received 9 August 2019, revised 21 November 2019

Accepted for publication 25 November 2019

Published 31 December 2019



CrossMark

Abstract

We propose a laminar-jet-discharging method to measure the interfacial tension of deformable surfaces such as soap bubbles. This method avoids the need to measure the small pressure difference inside and outside a soap bubble in a static state. By allowing the air in a soap bubble to discharge in a laminar flow state through a long tube, we show that the surface tension of the soap bubble is proportional to the rate of change of the fourth power of the bubble radius. Experimentally, we verify that this linear relationship is valid over a long period and thus can be measured with cameras at slow recording rates. Our method offers a straightforward and accurate way to measure the surface tension of soap bubbles using easy-to-obtain devices. In addition, we propose a new development of the pendant drop method based on the silhouette of the drop, which does not require any pressure transducer or computation of the second-order derivatives of the drop profile and hence is easier to implement and less sensitive to the accuracy of the drop profile determination. For pure liquids, results from the new pendant drop method compare well with standard values. This method is thus used to verify the laminar-jet-discharging measurements.

Keywords: surface tension, soap bubble, laminar pipe flow, bubble discharge, deformable surface

(Some figures may appear in colour only in the online journal)

1. Introduction

Liquid–gas interfaces are frequently encountered in daily life and in industrial applications, of which soap bubbles and soap films are common examples. Surface tension is the key parameter characterizing the physical properties of these interfaces. It is desirable to have a simple and accurate method for surface tension measurement.

A variety of techniques have been used to measure surface tension. These methods may be broadly divided into two

categories: static methods and dynamic methods according to whether the interface is at a static or a dynamic force balance.

Wilhelmy plate, Du Noüy ring, capillary-rise, drop volume and pendant drop methods are widely used examples of static methods [1, 2]. With the advance of the imaging technique, it is possible to quantitatively determine the shape of liquid drops resting on a surface or hanging on a capillary tube, which is the basis of measuring the surface tension and the contact angle using the sessile [3] or pendant drop methods [2]. The pendant drop method, which has a long history [4–8], is more popular as the solid boundaries are typically further away from the drop and hence it is easier to determine the drop surface profile from the image. Axisymmetric drop shape

⁴ Author to whom any correspondence should be addressed.

analysis (ADSA) algorithm [9] is widely used in this method. It consists of two steps. The first step is to detect the shape profile of the pendant drop, which is assumed to be axisymmetric. The second step is to solve the pressure balance equation with multivariable minimization algorithm under proper boundary conditions. Many methods have been proposed [10–12] to obtain the shape profile with high accuracy from digital images as the surface tension is very sensitive to the measurement error of the drop shape profile. Nevertheless, as the pressure balance equation involves the second order derivative of the drop shape, shape measurement error is a source of large uncertainty [13].

In all above methods, the interfaces are at equilibrium. There are, however, other examples in which the interfaces are in motion. For these systems, the dynamic methods can be used.

The maximum bubble pressure method is one such dynamic method that can be dated back to Schrödinger [15]. To understand this method, we start with a spherical soap bubble at equilibrium. For such a bubble, which have two liquid–gas interfaces, the Young–Laplace equation becomes:

$$\Delta P = \frac{4\sigma}{R}, \quad (1)$$

in which ΔP is the pressure difference inside and outside the bubble and R is the radius of the bubble. In principle, equation (1) can be used directly to obtain the surface tension by measuring the pressure difference, either using a pressure transducer or a liquid column, and measuring the size of the bubble using a camera. Note that this is still a static method. In this method [14, 16–19], on the other hand, the pressure differences are very small for bubbles with reasonable sizes, hence it is not easy to reach high accuracy in pressure measurements. In addition, as equation (1) indicates, the pressure difference decreases as bubble grows, which makes it difficult to generate a bubble and maintain it at desired size. In order to overcome the difficulties associated with the static method, it is proposed to measure only the maximum bubble pressure during the expansion of a bubble [16, 20]. As a gas is slowly injected through a small tube immersed in a liquid, a bubble will form and grow at the tip of the tube. The pressure inside and outside the bubble varies as the bubble grows. This pressure difference reaches a maximum when the bubble is hemispherical, at which its radius is the smallest and equals the inner radius of the tube. The surface tension can thus be obtained from equation (1) as the radius of the tube is known and the maximum pressure is measured. This method eliminates the need to measure the size of the bubble and the need to maintain the bubble at steady state. On the other hand, it needs to determine the maximum pressure of a time series and the gas injection process should be slow to avoid the transient effects.

In this paper, we propose a laminar jet-discharging method which obtains the surface tension by measuring the dynamic evolution of the radius of a soap bubble. We present the method below and compare its result with that from a new pendant drop method that gives an explicit measurement of surface tension, avoiding iteration and proper initialization as in more popular algorithms based on multivariable minimization. We

tested our pendant drop method against ADSA and the results are in good agreement. We show that the jet-discharging method has good accuracy and is easy to use, without the need of expensive equipment.

2. The method

2.1. Laminar-jet-discharging method

As we discussed above, previous methods to measure the surface tension of soap bubbles rely on the static pressure balance given by the Young–Laplace equation (1). The difficulty associated with this approach lies on the fact that the pressure difference is inversely proportional to the size of the bubble, which results in very small pressure differences that are hard to measure and to control accurately for bubbles with reasonable sizes.

Here we propose to utilize the Young–Laplace equation for a bubble that is discharging but the volume change is so slow that the bubble is in a quasi-static state. A simple mass balance of the bubble gives

$$\frac{dV}{dt} = \frac{d}{dt} \left(\frac{4\pi}{3} R^3 \right) = 4\pi R^2 \frac{dR}{dt} = -Q, \quad (2)$$

where R is the radius of the bubble and Q is the volume discharging rate of the bubble. In equation (2) we have assumed that the density of the air in the bubble is uniform and remains the same when it discharges from the bubble. This assumption will be justified later in the appendix.

Now the question is to maintain the volume discharging rate Q in a well-controlled manner. Our method is to let the bubble discharge through a long tube with a small diameter. For a tube that is long enough, the pressure difference across the tube, which is the same as the pressure difference inside and outside the soap bubble given by the Young–Laplace equation, drives a laminar flow in the tube. Again, if the size of the soap bubble varies slowly, the pressure difference changes slowly and the flow may be regarded as nearly steady. In that case, the volume flow rate through the tube is given by the well-known Hagen–Poiseuille solution:

$$Q = \pi r_0^2 \bar{U} = \pi r_0^2 \frac{r_0^2}{8\mu} \frac{\Delta P}{L}, \quad (3)$$

in which \bar{U} is the average air velocity in the tube, μ is the dynamic viscosity of air, r_0 and L are the inner radius and the length of the tube, respectively.

Combining equations (1)–(3), we obtain an equation for the evolution of the bubble radius

$$4\pi R^2 \frac{dR}{dt} = -\frac{\pi r_0^4}{2\mu L} \frac{\sigma}{R}, \quad (4)$$

which gives the instantaneous surface tension of the bubble in terms of the rate of change of the bubble radius

$$\sigma = -\frac{8\mu L R^3}{r_0^4} \frac{dR}{dt} = -\frac{2\mu L}{r_0^4} \frac{dR^4}{dt}. \quad (5)$$

If the surface tension remains constant during discharging, then this equation can be integrated to yield

$$R_0^4 - R^4(t) = \frac{r_0^4 \sigma}{2\mu L} t, \quad (6)$$

where $R_0 = R(t = 0)$ is the initial radius of the soap bubble. Equation (6) shows that for bubble with constant surface tension σ , $R^4(t)$ decreases linearly with time and the slope of the linear relationship is proportional to σ , which provides an easy way to measure the surface tension: with known tube radius r_0 , length L , gas viscosity μ , then measuring the bubble sizes at two different times $R_1 = R(t_1)$ and $R_2 = R(t_2)$ is enough to determine σ .

In the derivation above, we made several assumptions to simplify the derivation. In the appendix, we discuss in detail the conditions for these assumptions to be valid, and we show that for typical experiments with soap-bubbles, the examples shown in this work, all these assumptions indeed hold.

2.2. A new algorithm for the pendant drop method

To verify the jet-discharging method proposed here, we also measured the surface tension from the pendant drop method, but with a slightly different implementation. As shown in figure 1, if we consider the force balance of the lower part of the drop that has a height of z_1 above the bottom point, denoting the radius of the drop at height z as $r(z)$, we have

$$F_1 \cos(\theta_1) = (P_1 - P_a) \pi r_1^2 + G \quad (7)$$

where $F_1 = \sigma \cdot 2\pi r_1$ is the force along the interface on this part of the drop due to surface tension, P_a is the pressure of the atmosphere at the bottom point, P_1 is the pressure at $z = z_1$, and $G = \Delta\rho g \int_0^{z_1} \pi r^2(z) dz$ is the gravitational force on the lower part with $\Delta\rho$ the density difference between the soap solution and air and g the gravitational acceleration. We choose the coordinate z pointing upward with origin on the bottom point of the drop. Note that the relation between P_1 and P_a is not straightforward and is one of the uncertainties in previous pendant method. Here we note that the liquid pressure at any height is $P(z) = (P_0 - \Delta\rho g z)$. Substitute $P_1 = P_0 - \Delta\rho g z_1$ into equation (7), and note $\Delta P_0 = P_0 - P_a$, we obtain

$$F_1 \cos(\theta_1) = (\Delta P_0 - \Delta\rho g z_1) \pi r_1^2 + G. \quad (8)$$

This equation was used directly by Danov *et al* to measure the surface tension of pendant drops [8], in which a pressure transducer was used to measure ΔP_0 , the pressure difference at $z = 0$. The accuracy of the surface tension measurement thus depends on the accuracy of the pressure measurement, in addition to the accuracy of the drop profile measurement.

Here we propose a method that avoids the need to measure the pressure difference ΔP_0 . We note that if one divides equation (8) by πr_1^2 and applies it at two different heights z_1 and z_2 , then their difference does not depend on ΔP_0 . In that case we obtain,

$$\sigma = \frac{1}{2} \Delta\rho g \times \frac{z_1 - z_2 + r_2^{-2} \int_0^{z_2} r^2 dz - r_1^{-2} \int_0^{z_1} r^2 dz}{\left[r_2 \sqrt{(r'_z)^2 + 1} \right]^{-1} - \left[r_1 \sqrt{(r'_z)^2 + 1} \right]^{-1}} \quad (9)$$

in which we have used $\cos(\theta) = [1 + (r'_z)^2]^{-1/2}$, with $r'_z = dr/dz$, i.e. the slope of the profile of the drop. This equation can be used to determine the surface tension, and we note that the second derivative of $r(z)$ does not appear in it, which means that there is no need to perform high-order numerical differentiation, an operation that usually magnifies measurement error. It is worth mentioning that the analysis procedure proposed here can also be applied to the sessile drop method.

Next, we give a brief description of our experimental setup and the images of the bubble and the drop obtained from the experiments.

3. Experimental setup

Figure 2(a) shows a sketch of our experimental system. The bubble was created at the end of a long stainless tube with length L and inner radius r_0 . We tested three kinds of tubes with different lengths and radii: $L = 204$ mm and $r_0 = 0.765$ mm, $L = 204$ mm and $r_0 = 1.00$ mm, and $L = 500$ mm and $r_0 = 0.765$ mm. Our tests showed that all tubes ensured Hagen–Poiseuille flow inside and the results obtained from the different tubes are all consistent, which confirmed our theoretical analysis shown in the appendix. We chose the tube with intermediate L/r_0 ratio, i.e. the one with length $L = 204$ mm and inner radius $r_0 = 0.765 \pm 0.003$ mm, to carry out all the experiments reported here. The inner radius of the tube was determined by taking an image of the tube exit under a microscope. The inner edge of the tube was then detected using gradient edge detection method (using the Canny algorithm). The inner radius is then determined from least-square fitting of those edge pixels to a circle. The uncertainty in tube radius is estimated from the pixel size of the digital image. This uncertainty of 0.4% in r_0 gives an uncertainty of 1.6% in the measured surface tension, as indicated by equation (6). The bubble was first inflated with air up to a size of $R_0 \approx 15$ mm using a syringe pump. After waiting a few seconds for the air trapped in the bubble to settle, the syringe pump was detached and the bubble started to discharge through the tube.

To avoid possible effects on surface tension due to the variation of environment temperature, the bubble was placed in a constant-temperature chamber consisting of two glass container and a water jacket in between, as shown in figure 2(b). The water in the water jacket was continuously cooled by a cooling coil connected to a chiller. The water temperature was maintained constant by switching on/off an electric heater in the water jacket according to the water temperature. We conducted experiments for water temperature in the range of 10 °C–50 °C. At each temperature setting, the temperature

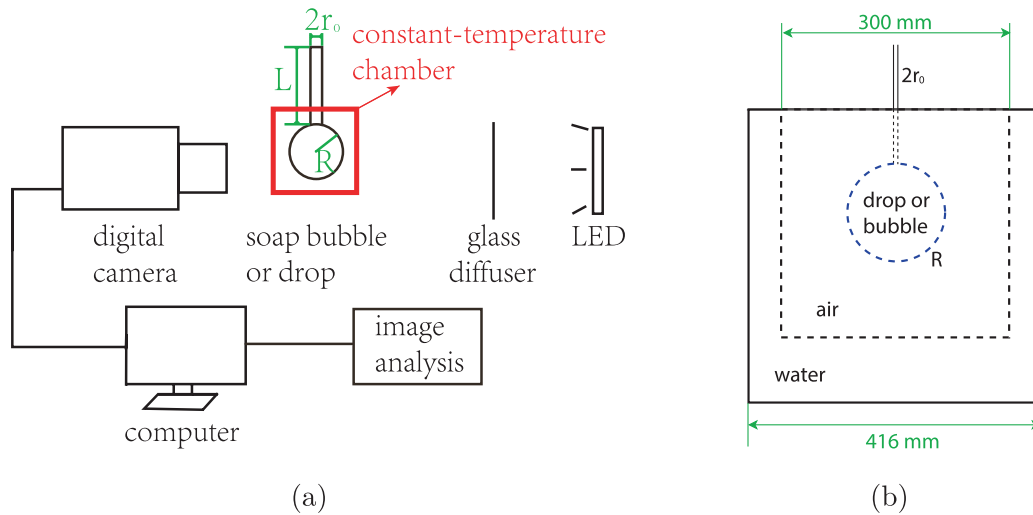


Figure 1. (a) Sketch of the experimental setup, including the LED light source, the ground glass diffuser, the soap bubble, the constant-temperature chamber, the digital camera, and the computer for image analysis. (b) The constant-temperature chamber consisted of two glass containers with a water jacket in between.

variation of the air in the chamber was maintained within $\pm 0.1\text{ }^\circ\text{C}$.

The soap solution is a mixture of pure water, glycerol, and the ‘Dawn’ detergent. The mass ratio of glycerol in the mixture was always at 10%, while the mass concentration of the detergent varied from $c_{\text{dawn}} = 2\%–32\%$, which corresponds to mole concentrations of sodium dodecyl sulfate (SDS), the effective surfactant in the detergent, from $c_{\text{SDS}} = 20\text{ mol m}^{-3}$ to 320 mol m^{-3} . We note that this concentration range for SDS is usually referred to as the ‘saturation range’, i.e. the surface tension of the solution does not change with the SDS concentration any more [21–23].

The deflating process of the soap bubble was illuminated by backlighting with an LED white light source and was recorded by a digital camera as shown in figure 2. To achieve homogeneous illumination, a ground glass diffuser was placed between the LED light source and the bubble. As shown in figure 3, the images of the bubble thus appear darker than the background, which facilitates subsequent image processing to measure the radii of the bubbles. The image was $2560 \times 1600\text{ px}$ with a spatial resolution of $33.3\text{ }\mu\text{m px}^{-1}$, and the camera frame rate was set to 10 frame s^{-1} at the beginning stage of the deflation and 20 frame s^{-1} in the later stage as the bubble size varies highly nonlinearly with time (because $R^4(t)$ is linear in time).

Figure 4 shows the experimental image of the pendant drop method. The drop is also darker than the background while the center of the drop is brighter as the drop works as a small lens and thus focuses light to its center. The pendant drop images were taken at $2560 \times 1600\text{ px}$ with a spatial resolution of $9.8\text{ }\mu\text{m px}^{-1}$. As the image is stationary, the camera frame rate is inessential and we used 24 frame s^{-1} for convenience. The surface tension were calculated by analyzing the shape of the drop edges on those images and using equation (9) given above.

To check the pendant drop method proposed here, we measured the surface tensions of water-air, ethanol-air and

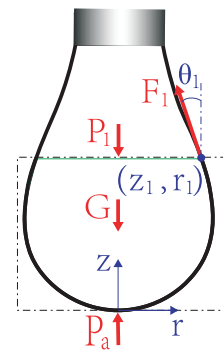


Figure 2. The force balance of the lower part of the drop.

glycerol–air interfaces, all at 30° . In each case, ten drops were recorded and their images analyzed to give the surface tension. The averaged values are shown in table 1, together with the reference values for the pure fluids [24, 25]. As a further check of our pendant drop method, we used the commercial software DSA4 from Krüss GmbH to analyze the same pendant drop images using the ADSA algorithm. The results are also shown in table 1. The error bars shown are the maximum deviations from the average among the ten different measurements. Table 1 shows that for these pure fluids, the results of our pendant drop method are in good agreement with those from DSA4 and with the reference values.

4. Experimental results and discussion

4.1. Result from bubble-discharging measurement

For each image of the deflating bubble, similar to those shown in figure 3, we performed gradient edge detection method (using the Canny algorithm) to identify the edge pixels of the soap bubble. By fitting those edge pixels with a circle using least-square-fit, we obtained the radius of the bubble at that

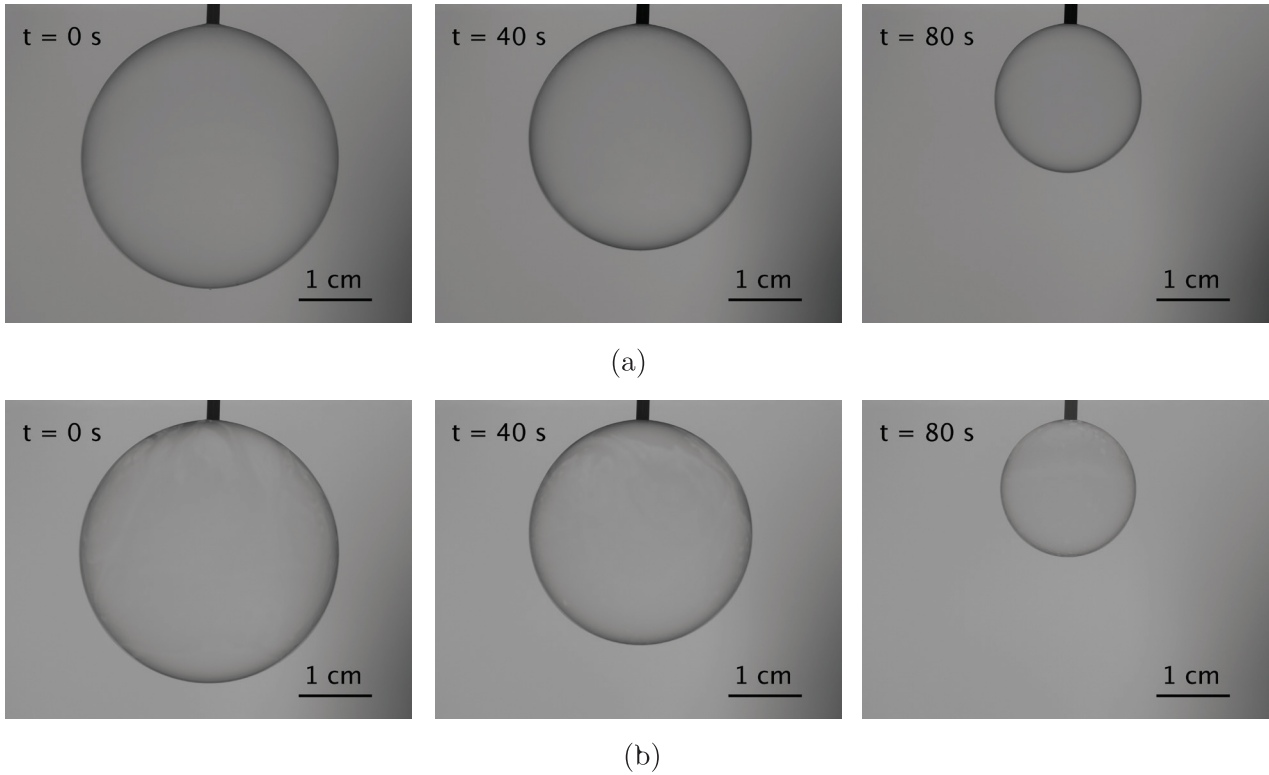


Figure 3. Experimental images of a deflating soap bubble at different time t of the discharging process. The concentration of the detergent in the soap solution is $c_{\text{dawn}} = 2\%$ for (a) and $c_{\text{dawn}} = 10\%$ for (b). The temperature of the air in the constant-temperature chamber is $T = 30\text{ }^{\circ}\text{C}$.

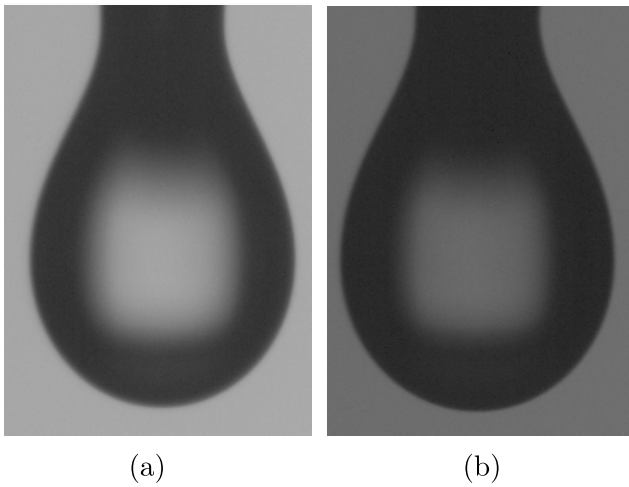


Figure 4. (a) An experimental image of the pendant drop at $c_{\text{dawn}} = 2\%$. (b) An experimental image of the pendant drop at $c_{\text{dawn}} = 16\%$.

Table 1. Measured interfacial tensions of pure liquids in air.

Interfaces	Ref. value (mN m^{-1})	DSA4 (mN m^{-1})	Equation (9) (mN m^{-1})
Water-air	71.2	70.0 ± 2.9	69.9 ± 2.0
Ethanol-air	21.4	21.3 ± 0.7	21.1 ± 0.3
Glycerol-air	62.8	63.4 ± 1.0	63.9 ± 2.2

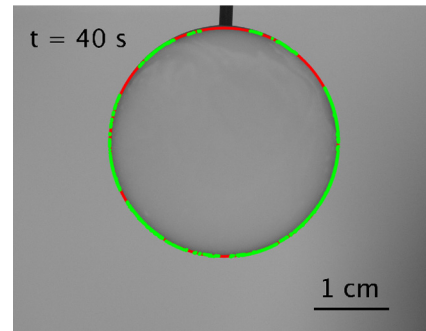


Figure 5. Identification and fitting the edge of the bubble for $c_{\text{dawn}} = 16\%$ at $t = 40\text{ s}$. The green dots are the points on the edge of the bubble and the red circle is the fitting result.

time, as shown in figure 5. We then plotted the change of bubble radius with time in the form of $R_0^4 - R^4(t)$ versus t as given by equation (6).

Figure 6(a) shows the data for bubbles with different detergent concentrations $c_{\text{dawn}} = 2\%$ and $c_{\text{dawn}} = 16\%$. In both cases, the experimental data lie on straight lines. Fitting the data with equation (6), and substituting in the known parameters r_0 , μ , and L , we obtained the surface tension of the air/soap-water interface at the given temperature and detergent concentration. In figure 6(b), we show the instantaneous surface tensions as calculated from equation (5) for the two cases, together with the constant surface tension that we measured

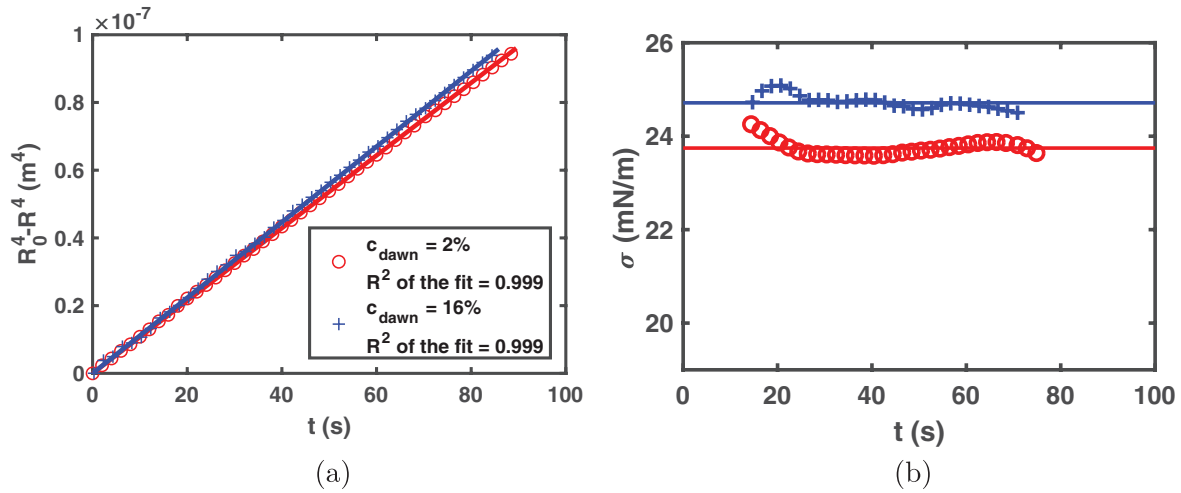


Figure 6. (a) Change of bubble radius with time, shown as $R_0^4 - R^4(t)$ versus t . The open circles (‘o’) and the pluses (‘+’) are for bubbles with detergent concentration $c_{\text{dawn}} = 2\%$ and $c_{\text{dawn}} = 16\%$, respectively. The solid lines are the least-square-fit of the data. For the two cases shown here, the bubble radii changes from approximately from 15 mm to 1.5 mm. (b) Measured instantaneous surface tension versus t for the two cases, which is calculated by equation (5) using the local derivative of dR^4/dt from the data shown in (a). The straight lines are the corresponding average values calculated using equation (6).

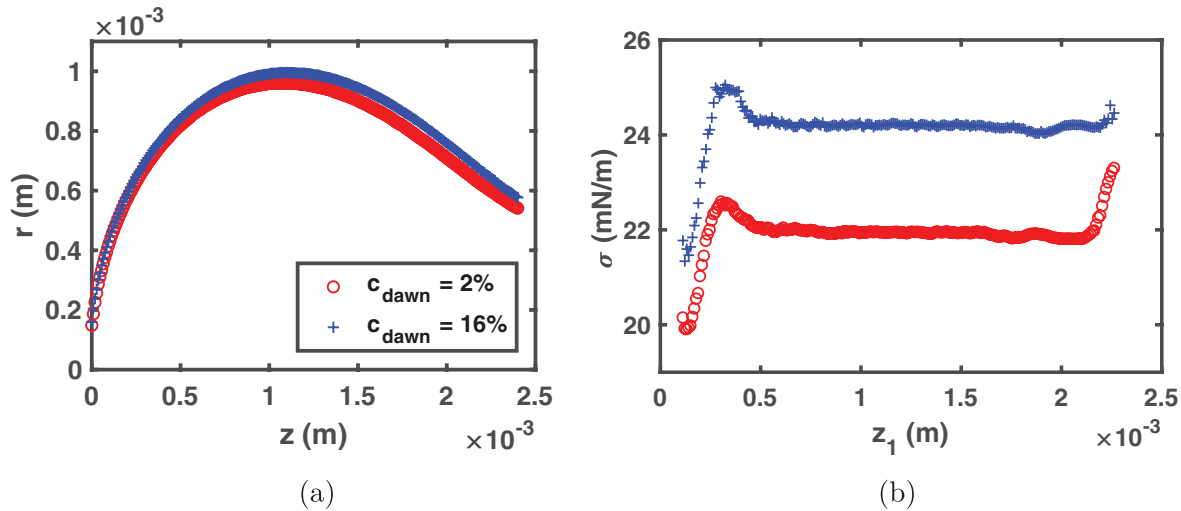


Figure 7. The green open circles (‘o’) symbols are the experimental data at $c_{\text{dawn}} = 2\%$ and the blue plus (‘+’) symbols is at $c_{\text{dawn}} = 16\%$. (a) The change of drop radius r with height z and (b) the surface tension versus $\Delta z = z_2 - z_1$ obtained by equation (9), where z_2 is fixed on the large z . Only the range 1/3–2/3 of z will be used to take average to obtain the surface tension.

from straight-line fitting using equation (6). The instantaneous dR^4/dt was obtained by performing a convolution operation of the measured $R^4(t)$ data with a Gaussian derivative kernel, which combines smoothing and differentiation [26].

4.2. Result from pendant drop measurement

For images of the pendant drops as shown in figure 4, we detected the edge of the drop and obtained the relation $r(z)$ versus z at steps of $\Delta z = 1 \text{ px} = 9.8 \text{ }\mu\text{m}$. As the drop size is typically a few millimeters, this resolution is very high, which allows us to compute the derivative $r'(z)$ by finite differences. Figure 7(a) shows the curves $r(z)$ for drops with detergent concentration $c_{\text{dawn}} = 2\%$ and $c_{\text{dawn}} = 16\%$. To calculate the surface tension σ from equation (9), we choose z_2 at a position

close to the rod end and varied z_1 . The results corresponding to the two cases of figure 7(a) are presented in figure 7(b) with respect to the position z_1 . Equation (9) gives a constant value of σ , independent of the value of $z_2 - z_1$. The results in figure 7(b) indicate that for small values of $z_2 - z_1$, the difference is very small so that measurement errors have a large effect, while for large values of $z_2 - z_1$, which is achieved by having small z_1 values, the end effect of the drop is significant because the derivative $r'(z)$ changes rapidly for small z (note that $r'(z) = \infty$ at $z = 0$) and hence it is difficult to measure accurately. However, for intermediate values of $z_2 - z_1$, the equation gives constant values independent of $z_2 - z_1$, which is the value we report here. For droplets the size of 2–3 mm, this range is approximately 0.5–1.5 mm, or roughly 1/3 of the drop size.

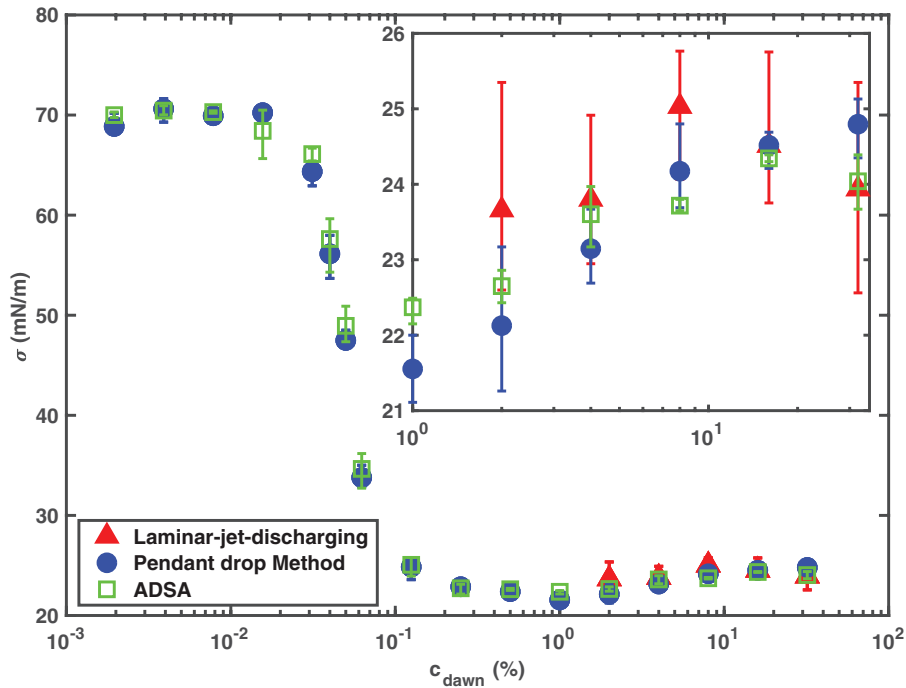


Figure 8. Surface tension measured by pendant drop method (blue circles ‘●’) using equation (9) and jet-discharging method (red triangles ‘▲’) using equation (6) and DSA4 software (green square ‘□’). The inset shows a magnification of the range of data over which the jet-discharging method was applied.

4.3. Discussion

In figure 8, we show the surface tension σ , measured from the laminar-jet-discharging method, the pendant drop method, and from the DSA4 software, over a wide range of the detergent concentration c_{dawn} . As the figure shows, the results of new pendant drop method are in good agreement with those of DSA4 over the entire range of surfactant concentration investigated. While the new pendant drop method and the DSA4 software were used for soap solutions at any detergent concentration, the bubble jet method was only used at $c_{\text{dawn}} \geq 2\%$, because it is difficult to generate a stable bubble at low surfactant concentration. For very dilute surfactant concentration, $c_{\text{dawn}} \leq 0.01\%$, σ approaches a constant value of $70 \pm 2 \text{ mN m}^{-1}$, which is close to but slightly less than 72 mN m^{-1} , the surface tension of pure water. When c_{dawn} increases from 0.1% to 2%, σ decreases very rapidly and then reaches another approximately constant value. Lin *et al* [22] also reported this behaviour of surface tension for SDS solutions when measured using a Wilhelmy plate surface tension meter. This variation of surface tension with surfactant concentration might be related to the formation of precipitates in the solution as reported in the experimental by Kralchevsky *et al* [27]. For detergent concentration higher than 2%, the surface tension measured from the jet-discharging method is nearly a constant at $\sigma \approx 24.5 \text{ mN m}^{-1}$, which is also the constant value given by the pendant drop method. We also found that it does not change with temperature. The results are consistent with measurements reported in [28, 29], which measured the surface tension by means of stalagmometric methodology and the pendant drop method, respectively. Our result is slightly lower than that found by Bianco *et al* [14] using the dynamic

maximum pressure method and by Sane *et al* [30] who measured the surface tension of flowing soap films. The values of surface tensions reported there are approximately 30 mN m^{-1} for SDS solutions in the saturated range. The surface tensions measured with the pendant drop method agree with the results from the jet-discharging method for higher concentration ($c_{\text{dawn}} \gtrsim 10\%$, or $c_{\text{SDS}} \gtrsim 100 \text{ mol m}^{-3}$). For lower concentrations, the results from the pendant drop method are slightly smaller than those from the jet-discharging method.

4.4. Outlook

In previous examples, we demonstrated the laminar-jet-discharging method with the case in which the surface tension of the bubble varies very little and can be treated as a constant, which corresponds to the situation when the surfactant in the solution is saturated. For lower concentrations of the surfactant, the surface tension could change with time during the deflation of the bubble as the surfactant concentration on the interfaces could vary with the surface area change. Then the value of $R_0^4 - R^4$ would not vary linearly with time. Figure 9(a) is an example of the measurement for a detergent concentration of $c_{\text{dawn}} = 0.5\%$, which is clearly nonlinear. With the help of high-speed imaging, our method is able to resolve the change of bubble radius with time, which then gives the instantaneous surface tension from dR^4/dt by equation (5) using the smoothing and differentiation algorithm [26], provided the simplifications discussed in appendix are still justified. The change of surface tension with time corresponding to the case in figure 9(a) is shown in figure 9(b). While the surfactant on the surface of the bubble is unsaturated, the concentration of surfactant will increase with the

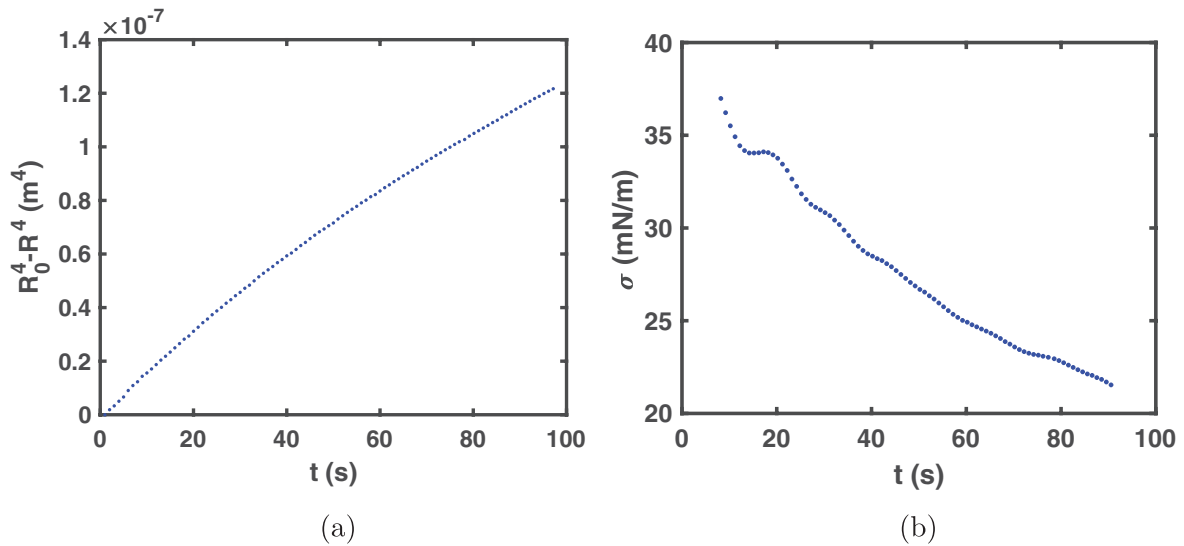


Figure 9. (a) The change of $R_0^4 - R^4(t)$ with time for a dilute soap solution with detergent concentration $c_{\text{dawn}} = 0.5\%$. In this case, the surfactant concentration is unsaturated and hence its surface concentration on the interface changes with the surface area, which results in a nonlinear dependence of $R_0^4 - R^4(t)$ with time. (b) Measured instantaneous surface tension, which decreases with time because the surfactant concentration on the bubble surface increases with time as the bubble deflates.

deflating of the bubble, which leads to the decrease of the surface tension. This type of measurement could reveal how surface tension changes with the film thickness of the bubble and hence would provide insight to distinguish whether the surfactant concentration on the bubble surface is described by the Gibbs relation or the Marangoni relation [31], which has been under intense debate [14, 23, 32–35]. This is a direction in research that our method could help to explore.

5. Conclusion

There have been experiments designed to measure surface tension by monitoring the pressure in the bubble when charging the bubble. Because the pressure is inversely proportional to bubble size, it is difficult to maintain a stable charging process for accurate measurement. Consequently, previous methods typically use only a single point at which the pressure reaches maximum [14, 17]. In this work, we proposed a method that utilizes a quasi-steady laminar discharging process that allows an analytical expression for the change of bubble size with time to be derived, which can be used to measure the surface tension. For soap bubbles, we discussed the conditions required for the discharging process to be laminar and quasi-steady and showed that it can be achieved with commonly available materials. This method can also be used to measure the interfacial tension of other deformable surfaces such as gas bubbles in liquids.

As an effort to validate the bubble-discharging method, we also measured the surface tension using the pendant drop method [2, 4–8, 13]. For this method, we introduced a new way of data processing that avoids calculating the second derivative of the drop profile and hence may produce results with higher accuracy. For detergent-water solutions with a range of detergent concentrations, the surface tensions measured with the pendant-drop method and the bubble-discharging method

and DSA4, are in good agreement with each other, and are consistent with data reported in the literature.

A notable feature of the bubble-discharging method is its simplicity to use—it does not require expensive devices. In our experiment, we verified the linear dependence of the change of the fourth power of bubble radius, $R_0^4 - R^4(t)$, with time. Therefore, there is no need to record the image at high frame rate. An ordinary CCD camera that can take pictures at 10 frame s^{-1} would be sufficient. In fact, the measurement can be done even with a common cellphone held still, without the need of any pressure measuring devices.

Acknowledgments

We are very grateful to Mr Linlin Fei for his valuable help in building the experimental apparatus, to Mr Wenhai Lei for his valuable help in calculating the surface tension using DSA4. This work is supported financially by Tsinghua University.

Appendix. Justification of the assumptions

To obtain equation (6), we made a few assumptions to simplify the derivation. Here we check the validity of these assumptions in typical experiments.

Incompressible flow

Our first assumption is that the density of air is nearly constant, or incompressible, in the entire system. This is because that for soap bubbles with sizes that are easily detectable, the pressure difference is much smaller than the pressure inside the bubble. For example, for a bubble with radius $R = 1 \text{ mm}$, the pressure difference is about $\Delta P = 4\sigma/R \lesssim 300 \text{ Pa}$ because the surface tension of soap bubbles is always smaller than that

of pure water/air interface $\sigma_w = 72 \text{ mN m}^{-1}$. Therefore, for an experiment conducted at constant temperature, the air density variation is merely

$$\frac{\Delta\rho}{\rho} = \frac{\Delta P}{P} \lesssim 0.3\%. \quad (\text{A.1})$$

Laminar flow

For the volume flow rate to be given by equation (3), the air flow in the tube should be laminar, which requires that the Reynolds number is below the critical Reynolds number

$$\text{Re} \equiv \frac{\rho \bar{U} 2r_0}{\mu} = \frac{\rho r_0^3}{4\mu^2} \frac{\Delta P}{L} = \frac{\rho r_0^3 \sigma}{\mu^2 L R} \leq \text{Re}_{\text{cr}}, \quad (\text{A.2})$$

where Re_{cr} is the critical Reynolds number below which the flow is laminar. For Hagen–Poiseuille flow, experimental evidences show that $\text{Re}_{\text{cr}} \approx 2040$ [36]. This requirement can be easily satisfied by choosing appropriate tube length L . For example, if we use a tube with radius $r_0 = 1 \text{ mm}$, then using a length $L = 200 \text{ mm}$ gives $\text{Re} \lesssim 1400$ for $\Delta P \approx 300 \text{ Pa}$, which corresponds to the pressure difference for a pure water bubble with radius $R = 1 \text{ mm}$, much larger than the pressure difference for soap bubbles with sizes used in actual experiments. We thus conclude that this assumption of laminar flow in the tube is valid, as long as we do not use tubes that are too short.

Quasi-steady flow

When using equation (3) to calculate the volume flow rate of air, we also assumed that the flow is quasi-steady flow, i.e. the change of the flow with time is very slow. To quantify this, we examine the momentum equation of the flow in the tube. If we ignore the entrance effect, the flow in the tube is unidirectional, i.e. everywhere the fluid velocity is parallel to the tube axis. In addition, because of the axisymmetry of the flow, the Navier–Stokes equation reduces to a simpler form

$$\frac{\partial U}{\partial t} = -\frac{1}{\rho} \frac{dP}{dx} + \frac{\mu}{\rho r} \frac{\partial}{\partial r} \left(r \frac{\partial U}{\partial r} \right) \quad (\text{A.3})$$

where $U(r, t)$ is the fluid velocity, which, in general, is a function of time t and the radial distance to the tube axis r , but does not depend on the streamwise location x . The pressure P , on the other hand, depends only on x and that pressure gradient drives the flow in the tube. If the flow is steady, e.g. a pipe flow driven by a constant pressure gradient, $\partial U/\partial t = 0$ and the pressure gradient, which is given by $dP/dx = -\Delta P/L$ balance the viscous drag, which gives the Hagen–Poiseuille solution. However, during the discharging process, because the radius of bubble is changing, the pressure difference, and hence the pressure gradient, is also changing with time. Therefore the flow velocity is varying. For the flow to be quasi-steady, the magnitude of the unstable term must be small compared to the pressure gradient. The former may be estimated as

$$\begin{aligned} \left| \frac{\partial U}{\partial t} \right| &\sim \left| \frac{d\bar{U}}{dt} \right| = \frac{r_0^2}{8\mu L} \left| \frac{\partial \Delta P}{\partial t} \right| \\ &= \frac{r_0^2}{8\mu L} \left| \frac{\partial}{\partial t} \left(\frac{4\sigma}{R} \right) \right| = \frac{\sigma r_0^2}{2\mu L R^2} \left| \frac{dR}{dt} \right|. \end{aligned} \quad (\text{A.4})$$

Now, using equations (3) and (A.4), we obtain the requirement

$$\left| \frac{\partial U}{\partial t} \right| \left/ \left| \frac{1}{\rho} \frac{dP}{dx} \right| \right. \sim \frac{\rho \sigma r_0^6}{64\mu^2 L R^4} = \frac{r_0^3}{64R^3} \text{Re} \ll 1. \quad (\text{A.5})$$

Comparing with equation (A.2), we see that the second equality in equation (A.5) shows that this requirement is equivalent to a constraint on the Reynolds number modified by the geometric factor r_0^3/R^3 .

Uniform pressure in the bubble

There is one more implicit assumption in our derivation of the formula used to measure the surface tension, which is that we assumed that the air pressure in the bubble is uniform and the bubble remains spheric. If the bubble discharge is too fast, then the air flow inside the bubble might be significant that necessitates a pressure difference in the bubble, which could invalidate equation (1). The maximum pressure difference inside the bubble is to accelerate the air in the bubble to the discharge speed, which could be estimated by the Bernoulli equation as

$$\delta P_b \sim \frac{1}{2} \rho \bar{U}^2 = \frac{1}{2} \rho \left(\frac{r_0^2 \Delta P}{8\mu L} \right)^2. \quad (\text{A.6})$$

If this pressure difference is much smaller than the pressure difference due to the surface tension of the bubble, then our derivation is valid. That is to say, we require

$$\frac{\delta P_b}{\Delta P} \sim \frac{1}{32} \frac{\rho r_0^3 \Delta P}{4\mu^2 L} \frac{r_0}{L} = \frac{r_0}{32L} \text{Re} \ll 1. \quad (\text{A.7})$$

Spherical bubbles

In our analysis, we also assumed that the bubble is spherical during the entire process. As pressure itself is uniform as we discussed above, the only other mechanism that could break the spherical symmetry is gravity. If the gravitational force acting on the bubble is much smaller than the surface tension force, then the gravity effect is negligible. For a soap bubble, this effect could be made quantitative by the Bond number

$$\text{Bo} \sim \frac{\rho g R h}{\sigma} \sim \frac{\rho g R^2 h}{\sigma R} \sim \frac{\rho g V}{\sigma R} \quad (\text{A.8})$$

in which g is the gravitational acceleration, h is the thickness of the bubble and V is the volume of the soap-solution droplet before blowing the bubble. The critical Bond number may be estimated from the situation when gravitational force on the bottom half of the bubble exactly equals the surface tension force, i.e.

$$\frac{1}{2} \rho g V = 2\sigma 2\pi R, \quad (\text{A.9})$$

which gives

$$Bo_{cr} \equiv \frac{\rho g V}{\sigma R} = 8\pi. \quad (\text{A.10})$$

In our experiments, V is about 5 mm^3 . Therefore, Bo varies from approximately 0.1–1 for bubble radius decreasing from 20 mm to 2 mm, which is much smaller than Bo_{cr} . Hence the gravitational force should not cause much deformation of the bubble. It is also verified from our measurement—the bubble images are almost perfectly circular.

ORCID iDs

Dongmei Wan  <https://orcid.org/0000-0001-5667-0415>

Haitao Xu  <https://orcid.org/0000-0002-2863-7658>

References

- [1] Drelich J, Fang C and White C L 2002 Measurement of interfacial tension in fluid-fluid systems *Encyclopedia of Surface and Colloid Science* (New York: Marcel Dekker) pp 3158–63
- [2] De Gennes P G, Brochard-Wyart F and Quéré D 2004 *Capillarity and Gravity* (Berlin: Springer)
- [3] Del Rio O I and Neumann A W 1997 Axisymmetric drop shape analysis: computational methods for the measurement of interfacial properties from the shape and dimensions of pendant and sessile drops *J. Colloid Interface Sci.* **196** 136–47
- [4] Andreas J M, Hauser E A and Tucker W B 1938 Boundary tension by pendant drops *J. Phys. Chem.* **42** 1001–19
- [5] Adamson A W and Gast A P 1967 *Physical Chemistry of Surfaces* (New York: Interscience)
- [6] Stauffer C E 1965 The measurement of surface tension by the pendant drop technique *J. Phys. Chem.* **69** 1933–8
- [7] Hansen F K and Rødsrud G 1991 Surface tension by pendant drop: I. A fast standard instrument using computer image analysis *J. Colloid Interface Sci.* **141** 1–9
- [8] Danov K D, Stanimirova R D, Kralchevsky P A, Marinova K G, Alexandrov N A, Stoyanov S D, Blijdenstein T B and Pelan E G 2015 Capillary meniscus dynamometry—method for determining the surface tension of drops and bubbles with isotropic and anisotropic surface stress distributions *J. Colloid Interface Sci.* **440** 168–78
- [9] Saad S M I and Neumann A W 2016 Axisymmetric drop shape analysis (ADSA): an outline *Adv. Colloid Interface Sci.* **238** 62–87
- [10] Atae-Allah C, Cabrerizo-Vílchez M, Gómez-Lopera J F, Holgado-Terriza J A, Román-Roldán R and Luque-Escamilla P L 2001 Measurement of surface tension and contact angle using entropic edge detection *Meas. Sci. Technol.* **12** 288–98
- [11] Cabezas M G, Montanero J M and Ferrera C 2007 Computational evaluation of the theoretical image fitting analysis-axisymmetric interfaces (TIFA-AI) method of measuring interfacial tension *Meas. Sci. Technol.* **18** 1637–50
- [12] Favier B, Nikolaos T C and Athanasios G P 2017 A precise goniometer/tensiometer using a low cost single-board computer *Meas. Sci. Technol.* **28** 125302
- [13] Berry J D, Neeson M J, Dagastine R R, Chan D Y C and Tabor R F 2015 Measurement of surface and interfacial tension using pendant drop tensiometry *J. Colloid Interface Sci.* **454** 226–37
- [14] Bianco H and Marmur A 1993 Gibbs elasticity of a soap bubble *J. Colloid Interface Sci.* **158** 295–302
- [15] Schrödinger E 1915 Notiz über den Kapillardruck in Gasblasen *Ann. Phys., Lpz.* **351** 413–8
- [16] Mysels K J 1990 The maximum bubble pressure method of measuring surface tension, revisited *Colloids Surf.* **43** 241–62
- [17] Román F L, Faro J and Velasco S 2001 A simple experiment for measuring the surface tension of soap solutions *Am. J. Phys.* **69** 920–1
- [18] Fainerman V B, Miller R and Joos P 1994 The measurement of dynamic surface tension by the maximum bubble pressure method *Colloid Pol. Sci.* **272** 731–9
- [19] Kim Y H, Koczko K and Wasan D T 1997 Dynamic film and interfacial tensions in emulsion and foam systems *J. Colloid Interface Sci.* **187** 29–44
- [20] Kloubek J 1972 Measurement of the dynamic surface tension by the maximum bubble pressure method IV. Surface tension of aqueous solutions of sodium dodecyl sulfate *J. Colloid Interface Sci.* **41** 17–22
- [21] de Castro F H-B, Galvez-Borrego A and Hoces M C 1998 Surface tension of aqueous solutions of sodium dodecyl sulfate from 20 °C to 50 °C and pH between 4 and 12 *J. Chem. Eng. Data* **43** 717–8
- [22] Lin S Y, Lin Y Y, Chen E M, Hsu C T and Kwan C C 1999 A study of the equilibrium surface tension and the critical micelle concentration of mixed surfactant solutions *Langmuir* **15** 4370–6
- [23] Prins A, Arcuri C and Tempel M V D 1967 Elasticity of thin liquid films *J. Colloid Interface Sci.* **24** 84–90
- [24] Vazquez G, Alvarez E and Navaza J M 1995 Surface tension of alcohol water + water from 20 °C to 50 °C *J. Chem. Eng. Data* **40** 611–4
- [25] Takamura K, Fischer H and Morrow N R 2012 Physical properties of aqueous glycerol solutions *J. Pet. Sci. Eng.* **98** 50–60
- [26] Mordant N, Crawford A and Bodenschatz E 2004 Experimental Lagrangian acceleration probability density function measurement *Physica D* **193** 245–51
- [27] Kralchevsky P A, Danov K D, Pishmanova C I, Kralchevska S D, Christov N C, Ananthapadmanabhan K P and Lips A 2007 Effect of the precipitation of neutral-soap, acid-soap, and alkanolic acid crystallites on the bulk pH and surface tension of soap solutions *Langmuir* **23** 3538–53
- [28] Singh A, Sharma A, Bansal S and Sharma P 2018 Comparative interaction study of amylase and surfactants for potential detergent formulation *J. Mol. Liq.* **261** 397–401
- [29] Bonfillon A, Sicoli F and Langevin D 1994 Dynamic surface tension of ionic surfactant solutions *J. Colloid Interface Sci.* **168** 497–504
- [30] Sane A, Mandre S and Kim I 2018 Surface tension of flowing soap films *J. Fluid Mech.* **841** R2
- [31] Couder Y, Chomaz J M and Rabaud M 1989 On the hydrodynamics of soap films *Physica D* **37** 384–405
- [32] Georgieva D, Cagnab A and Langevina D 2009 Link between surface elasticity and foam stability *Soft Matter* **5** 2063–71
- [33] Karakasheva S I, Tsekov R, Maneva E D and Nguyen A V 2010 Elasticity of foam bubbles measured by profile analysis tensiometry *Colloids Surf. A* **369** 136–40
- [34] Kovalchuka V I, Makievskib A V, Kragel J, Pandolfinid P, Logliod G, Loglio G, Liggieri L, Ravera F and Miller R 2005 Film tension and dilational film rheology of a single foam bubble *Colloids Surf. A* **261** 151–21
- [35] Lucassen-Reynders E H, Cagna A and Lucassen J 2001 Gibbs elasticity, surface dilational modulus and diffusional relaxation in nonionic surfactant monolayers *Colloids Surf. A* **186** 63–72
- [36] Avila K, Moxey D, de Lozar A, Avila M, Barkley D and Hof B 2011 The onset of turbulence in pipe flow *Science* **333** 192–6